

Published in final edited form as:

*Biosens Bioelectron.* 2011 January 15; 26(5): 1815–1824. doi:10.1016/j.bios.2010.09.030.

## New trends in instrumental design for surface plasmon resonance-based biosensors

Abdennour Abbas, Matthew J. Linman, and Quan Cheng\*

Department of Chemistry, University of California, Riverside, California 92521, USA

### Abstract

Surface plasmon resonance (SPR)-based biosensing is one of the most advanced label free, real time detection technologies. Numerous research groups with divergent scientific backgrounds have investigated the application of SPR biosensors and studied the fundamental aspects of surface plasmon polaritons that led to new, related instrumentation. As a result, this field continues to be at the forefront of evolving sensing technology. This review emphasizes the new developments in the field of SPR-related instrumentation including optical platforms, chips design, nanoscale approach and new materials. The current tendencies in SPR-based biosensing are identified and the future direction of SPR biosensor technology is broadly discussed.

### Keywords

Surface plasmon resonance; SPR imaging; Optical sensor; Biochip design; Biosensor; Label-free detection

## 1. Introduction

Surface plasmons polaritons (SPP) are traveling charge density waves at the surface of conducting materials. Surface plasmons resonance (SPR) is a collective oscillation of these free charges (conduction electrons) present at the interface of two media (metal-dielectric) with permittivities of opposite sign. This resonance stems from the interaction of light with the free electrons under certain conditions. The SPP oscillations are associated with an electric field propagating along a metal-dielectric interface and decaying exponentially in the perpendicular direction. Most of the energy is then confined to the metal surface which explains the remarkable sensitivity of SPR to changes in optical parameters at the metal-dielectric boundary. Three characteristics of SPR are particularly relevant for any new sensor chip or optical platform design: (i) enhancement of the electric field, (ii) propagation length and (iii) penetration depth. We describe here briefly these properties for a more thorough understanding of the challenges behind some of the new designs described later:

### (i) Electric field enhancement

At the resonance angle, the intensity of the electric field at the interface between the metal and a dielectric is strongly enhanced compared to that of the other side of the metal (Fig. 1). This is due mainly to the smaller complex permittivity in the dielectric compared to that in

\*Corresponding author: quan.cheng@ucr.edu, Tel: (951) 827-2702, Fax: (951) 827-4713.

**Publisher's Disclaimer:** This is a PDF file of an unedited manuscript that has been accepted for publication. As a service to our customers we are providing this early version of the manuscript. The manuscript will undergo copyediting, typesetting, and review of the resulting proof before it is published in its final citable form. Please note that during the production process errors may be discovered which could affect the content, and all legal disclaimers that apply to the journal pertain.

the metal (Ekgasit et al. 2004), and depends mostly on the thickness and optical properties of the materials. We will see that this enhancement can be multiplied by several techniques.

### (ii) Propagation length

The wavevector  $k$  of light propagating in a medium  $i$  of relative permittivity  $\varepsilon_i$  is given by:

$$k = \frac{\omega}{c} \sqrt{\varepsilon_i} \quad (1)$$

where  $\omega$  is the angular frequency and  $c$  the speed of light.

When the medium is free space, the wavevector becomes  $\omega/c$  or  $2\pi/\lambda_0$ , with  $\lambda_0$  being the incident wavelength. In the case of SPP, the propagation occurs along the interface between two semi-infinite media, here a gold film and a dielectric layer. The in-plane component of the wave vector  $k_{\text{SPP}}$  or dispersion relation (dependence of  $k_{\text{SPP}}$  on the angular frequency  $\omega$ ) is expressed as (Hornauer et al. 1974; Raether 1988):

$$k_{\text{SPP}} = \frac{\omega}{c} \sqrt{\frac{\varepsilon_m \varepsilon_d}{\varepsilon_m + \varepsilon_d}} \quad (2)$$

where  $\varepsilon$  is the dielectric permittivity and the subscript  $m$  and  $d$  refer to the metal and contacting dielectric medium, respectively. The dielectric permittivity of the metal is a complex quantity:  $\varepsilon_m = \varepsilon_m' + \varepsilon_m''$ . As a result, the SPP wave vector has a complex nature. This complex wavevector is then given as:  $k_{\text{SPP}} = k_{\text{SPP}}' + k_{\text{SPP}}''$ . The imaginary part ( $k_{\text{SPP}}''$ ) represents the SPP wave attenuation by metal absorption and radiative losses (Ekgasit et al. 2005; Kretschmann and Raether 1968b). This implies that the field intensity decays with a characteristic distance of  $1/2k_{\text{SPP}}''$ , which defines the SPP propagation length  $\delta_{\text{SPP}}$  as:

$$\delta_{\text{SPP}} = \lambda_0 \frac{(\varepsilon_m')^2}{2\pi\varepsilon_m''} \sqrt{\left(\frac{\varepsilon_m' + \varepsilon_d}{\varepsilon_m \varepsilon_d}\right)^3} \quad (3)$$

For  $\lambda_0 = 648$  nm, the SPP propagation length along the gold ( $\varepsilon_m = -12.57 + 1.21i$ )-air interface is  $17.4 \mu\text{m}$  and  $6.6 \mu\text{m}$  for the gold-water interface. These values represent the first limitation for SPR imaging resolution.

### (iii) Penetration depth

In addition to  $k_{\text{SPP}}$  which is the component parallel to the plane of propagation, the total wavevector  $k$  of the EM field at the metal-dielectric interface contains a second component  $k_z$  in the direction perpendicular to the interface. Its amplitude is expressed following the momentum conservation law and the Pythagorean theorem as shown here:

$$k^2 = k_{\text{SPP}}^2 + k_z^2 \quad (4)$$

The wavevector amplitude  $k_{z_i}$  is imaginary ( $|k_{\text{SPP}}| > |k|$ ) and thus expresses the exponential decay of the EM field in the  $z$  direction. The penetration depth  $\delta_i$  is then defined as the distance in the perpendicular direction to the interface at which the intensity of the EM field inside the medium  $i$  (metal or dielectric) falls to  $1/e$  (c.a 37 %) compared to the boundary at which the field was generated. It is expressed by combining equation (Williams) and (4) as:

$$\delta_i = \frac{\lambda_0}{2\pi} \sqrt{\left| \frac{\epsilon'_m + \epsilon_d}{\epsilon_i^2} \right|} \quad (5)$$

where  $\epsilon'_m$  the real part of the dielectric function of the metal layer,  $\epsilon_d$  the dielectric function of the contacting dielectric medium, and  $\epsilon_i$  refers here to  $\epsilon'_m$  or  $\epsilon_d$  depending on the direction considered for the decaying EM field. This equation shows that for  $\lambda_0 = 648$  nm and a gold film ( $\epsilon_m = -12.57 + 1.21i$ ) as the SPP carrying substrate, penetration depth is 191 nm in water, 351 nm in air, and only 27 nm inside the gold layer. These distances could be widely extended using specific designs, or exploited to generate new coupling schemes.

Most of the efforts on instrumental design aim principally to take advantage of the behavior of the three SPP properties presented above in different experimental conditions including the use of different excitation wavelengths, materials, geometry and assay environment.

Although the first observation of surface plasmons was reported more than a century ago (Wood 1902), the interest in this phenomenon was opened up by the connection made with the attenuated total reflection method (Kretschmann and Raether 1968a; Otto 1968), which enabled the optical excitation of surface plasmons. The use of SPR for sensing applications was first reported by the group of Raether who monitored the surface roughness of thin films by angular interrogation (Hornauer et al. 1974; Kapitza 1976). The following year, Gordon and Swalen (Gordon and Swalen 1977) measured the optical constants of organic monolayers from the SPR angular shift. Later, Lundstrom and coworkers (Liedberg et al. 1983) redefined the concept of SPR measurement by demonstrating the detection of gaseous analytes and biomolecules, and started the new era for this label-free technique. Since these pioneering works, SPR-based biosensors have become a competitive tool in analytical chemistry, bioanalysis, material and surface science. Particularly, the last decade has witnessed a constant technical improvement of both the instruments and methods used to generate, amplify or couple the SPR signal.

The fundamentals, physics, surface functionalization and applications of these sensors has already been extensively discussed in several reviews (Hoa et al. 2007; Phillips and Cheng 2007); (Abdulhalim et al. 2008; Homola 2008; Scarano et al. 2010; Willets and Van Duyne 2007). Besides the chemical interface and bio-functionalization, the SPR biosensor performance is highly dependant on the optical, electrical and structural features of the instruments. Here, we review the most relevant contributions and the recent advancements in the field of instrumental design for SPR biosensors, with a focus on ATR-based methods and planar configurations. The description of the new designs related to the different aspects and components is mainly organized following the important aspects in a typical SPR experiment: the optical excitation and transduction, the structural design and finally the biosensor assay environment. First, we discuss the design development based on new physical concepts for SPR excitation, propagation and coupling. We then analyze the structural design by discussing the importance of scale in SPR biosensors, even for sample volume miniaturization (microfluidics) or transducer miniaturization (micro/nanostructures). The structural design also concerns the use of new materials for specific biosensing properties. This is followed by a discussion on the optical and electronic environment of the SPR sensors and possible combinations with other instruments. Finally, we will offer our viewpoints on the future of SPR-based detection technologies in the biosensor field.

## 2. New excitation and wave coupling schemes

The resonant excitation of SPP in their propagative (in planar films) or localized (in metallic nanostructures) form is usually achieved by optical excitation through coupling devices. On planar metal-dielectric interfaces, the wavevector of surface plasmons polaritons is larger than that associated with the incident light beam. Hence, the excitation of SPP modes requires a prior enhancement of the component of light's wavevector that is parallel to the interface to match that of surface plasmons, which defines the matching condition as (Raether 1988):

$$k_{\text{spp}} = \frac{2\pi}{\lambda_0} \sqrt{\left(\frac{\epsilon_m \epsilon_d}{\epsilon_m + \epsilon_d}\right)} = \frac{2\pi}{\lambda_0} n_p \sin \theta_i \quad (6)$$

where  $n_p$  is the refractive index of the coupling prism and  $\theta_i$  is the incident angle of light.

This enhancement is mainly achieved by wave diffraction in grating structures, total internal reflection in a prism coupler, or a dielectric waveguides such as optical fibers (Fig. 2). Prism couplers used in the Kretschmann configuration are the most commonly employed in SPR spectroscopy (Kretschmann and Raether 1968a).

Several other techniques have been proposed for matching the momentum of the incident light to that of the SPs mode. The most recent include the free space excitation of propagating surface plasmons on gold films by nonlinear four-wave mixing using two incident beams in a modified Kretschmann configuration (Palomba and Novotny 2008). In addition, the coupling by light diffraction using a PDMS grating stamp has been reported (Kocabas et al. 2006), along with the excitation of localized SPs by optical vortex beams at normal incidence on a metal surface (Tan et al. 2008).

Beyond the use of the visible wavelength regime, the use of other regions of the EM spectrum for SPs excitation has also been investigated. One of the first studies in this topic was carried out by Hibbins et al. (Hibbins et al. 1999) at microwave frequencies a decade ago. They have reported the coupling of microwave radiation to surface plasmons using periodic structures and reflection measurements. Similar studies have been conducted in the infrared spectrum (Mertens et al. 2004). Recently, the excitation of SPs by a collimated beam of polychromatic light incident on a diffractive structure was reported (Telezhnikova and Homola 2006). This setup simultaneously performs SPs excitation and light dispersion over a position-sensitive detector.

During the last few years, increasing focus has been placed on the TeraHertz (THz) frequency range as well. This area of the electromagnetic spectrum has already been used in label free biodetection techniques since biomolecules have their collective vibrational and rotational modes in this band (Abbas et al. 2009a; Abbas et al. 2009b; Treizebre and Bocquet 2008; Treizebre et al. 2008). The exploitation of THz surface plasmons opens up possible new developments in this field. The difference between THz and optical SPP arises from different refractive indices of metals at the two frequency ranges. For instance, the refractive index of gold is larger than its values at visible frequencies by an order of  $10^3$ . Assuming a system composed of air as a dielectric and gold ( $n=0.553 \times 10^3 + i 0.654 \times 10^3$ , at 1 THz or  $\lambda = 300 \mu\text{m}$ ) as a resonant metal, the penetration depth into the dielectric, which is the crucial parameter in biosensing and imaging is  $\sim 2.7$  cm. This high value offers a high sensitivity for detection in the bulk medium but it also means that the SPs are weakly bounded to the metal-dielectric interface and most of the field is confined in the dielectric medium. The latter has a very low imaginary part of the refractive index and thus results in

minimal energy loss during propagation. Consequently, the propagation length is highly increased to reach a factor of  $10^5$  of the wavelength, which represents a drawback for SPR imaging resolution. However, this high propagation length could be a very interesting advantage if it is used for SPs enhancement by Bragg reflection. The back reflection of SP waves using periodic structures leads to constructive interference which multiplies the SPR signal in desired areas or spots. Hence, high image contrast and enhanced sensitivity could be obtained.

Another consequence of the low loss character of surface plasmons at THz frequencies is that metals cannot be used for guiding confined SPP in this band. This is expected since the plasma frequency for metals resides in both the visible and ultraviolet frequency regimes. Hence, the THz band requires new active or structured materials with a low plasma frequency to support plasmon excitation. Periodically nanostructured thin films or metamaterials (Pendry et al. 2004), ferroelectric semicrystalline polymers (Hassani et al. 2008), doped semiconductors (Grant et al. 2010; Xiaohua et al. 2009) and nanoporous silicon layers (Lo and Murphy 2010) have been proposed for this purpose.

Besides the investigation of different excitation light frequencies, the SPs excitation by s-polarized light has also been reported (Jen and Liao 2009; McMillan et al. 2005). Surface plasmons resonance could be excited either by p-polarized light or transverse magnetic (TM) waves when permittivities of the two adjacent media have opposite signs or by s-polarized light or transverse electric (TE) waves when permeabilities of the two adjacent media have opposite signs. For noble metals at optical frequencies, surface plasmons are associated with a p-polarized wave and thus could not be excited by TE waves. The excitation always requires a polarization conversion in an intermediate anisotropic layer before the light beam reaches the resonant metal. The unique approach to excite SPs with TE waves without a conversion layer is achieved through the use of negative index metamaterials as will be discussed later.

The development of new coupling schemes for SPR mainly focuses on the modification of the Kretschmann configuration as a means to enhance the resonance intensity or to integrate additional propagating modes. The most important of these designs are represented in Table 1. The addition of a dielectric layer supporting a waveguide mode in waveguide-coupled SPR (WCSPR) (Kovacs and Scott 1977) and plasmon-waveguide resonance (PWR) (Salamon et al. 1997) biosensors may enhance the EM field intensity by 50% and generate a sharp dip in the reflectivity spectrum (Salamon et al. 1997). This result indicates a high signal to noise ratio and improved resolution over conventional SPR spectroscopy based on noble metal substrates. Furthermore, the combination of both the waveguide and SP resonance modes enables the investigation of both TE and TM reflectivity spectra. This duality is particularly attractive for two kinds of applications: the analysis of the optical properties of anisotropic materials such as lipid bilayer membranes, thin films or self assembled monolayers by studying their birefringence and optical dichroism (Salamon and Tollin 2001); and the use of the bulk of the waveguiding layer as a 3-D matrix for analyte attachment. The latter offers the possibility of exploiting the guided mode resonance inside the waveguiding layer where the intensity reaches its maximum (Lau et al. 2004; Zhang et al. 2010). In the case of long range SPR configurations, the energy loss is greatly reduced and the SP propagation length highly increased (Sarid 1981). As a consequence, the sensitivity is higher than that of the previously cited designs. However, this configuration requires a symmetric environment on both sides of the metal layer, which is not easy to satisfy with some experimental conditions. Despite the abundant literature on the sensitivity of different SPR biosensors, rare studies were dedicated to the direct sensitivity comparison of different configurations. An interesting theoretical study was reported by Chien *et al.* a few years ago (Chien and Chen 2004). However, experimental investigations with the same SPR

instruments and under the same conditions are required to establish the actual performance of each design.

### 3. Microfluidics and microsystems for integrated SPR chips

Most of the efforts to integrate microfluidic microsystems to surface plasmon resonance are dedicated to the imaging approach. The basic principle is the fabrication of a microfluidic circuit in one substrate, generally glass or poly(dimethylsiloxane) (PDMS), followed by the bonding with a second glass substrate supporting the SPR-carrying metal. The aims of such integration are usually surface micropatterning, multiplexed analyte detection and/or fluid monitoring.

During the last few years, our group has investigated several surface micropatterning designs on planar gold substrates using PDMS microchannels for tethered lipid bilayer arrays (Taylor et al. 2009; Taylor et al. 2007) and DNA-protein/protein-protein interactions (Dong et al. 2008; Wang et al. 2007). The confinement of the samples inside the microchannels enabled a detection limit of immunoglobulin IgG in the nanomolar range (Fig. 3). PDMS-based microfluidics was also used by other groups (Lee et al. 2007; Luo et al. 2008). The use of microchannels significantly reduces the reaction time and sample consumption. Additionally, SPR imaging allows for real-time detection of the reaction occurring inside the microchannel. A number of groups used the microfluidic platform to decrease the nonspecific binding and instrument drift by internal referencing for individual flow cells in a parallel processing microfluidic network (Amarie et al. 2010; Eddings et al. 2009; Liu et al. 2009). One group recently reported the fabrication of a 1  $\mu\text{m}$  diameter SPR microcavity with a detection limit  $10^6$  times smaller than classical SPR biosensors (Amarie et al. 2010). Natarajan et al. reported a three-dimensional microfluidic system to deposit protein samples within discrete micrometric spots on a designed surface area (Natarajan et al. 2008). Using this technique, samples could be introduced in a continuous flow, allowing for the exposure of spots to a sufficient volume of sample.

Multiplexed detection using microfluidics aims essentially to minimize detection time by interrogation of multiple ligand/analyte interactions in a single device. Many developments have been reported this year for a wide variety of applications including biomolecular interaction monitoring (Krishnamoorthy et al. 2010), pathogen detection (Zordan et al. 2010) and analyte concentration measurement (Ouellet et al. 2010). The detection of nucleic acid at the femtomole scale using a microfluidic chip has been reported as well (Springer et al. 2010).

Electrowetting-on-dielectric (EWOD) is another microfluidic technique applied to SPR biosensors. The Tabrizian group reported the use of EWOD digital microfluidics for direct SPR chip functionalization by different DNA probes (Malic et al. 2009b). This method enables not only the immobilization at the designated detection sites, but the control of the immobilized probe density and orientation as well. This is achieved by applying a potential using the electric interface of the EWOD device. They also applied the same combination for a multichannel detection system (Malic et al. 2009a). In another work, a surface acoustic wave was tailored to a droplet-based SPR system (Galopin et al. 2007). Working with droplets rather than direct flow has the advantage of improving the accuracy of kinetic parameters measurements in the mass transport-limited regime. In addition to conventional SPR, microfluidic microsystems were also applied to localized SPR (Hiep et al. 2008; Huang et al. 2009).

Despite the increasing focus on array fabrication, the main challenge remains in the determination of the easiest and most cost-effective way to achieve a high degree of



parallelization for both analyte detection and biointeraction monitoring for high-throughput SPRi-based analysis. More efforts are expected in this direction in the future.

#### 4. Understanding the nanoscale effects on surface plasmons

Nanoscale research for SPR applications is essentially focused on optics studies of nanostructures and signal enhancement using nanomaterials. The theoretical and experimental verification of the nanostructures effects on SPs has become a major topic in photonics studies, giving rise to the new concept of nanoplasmonics. Particularly, two important works have inspired new technological developments for SPR biosensing: The demonstration of the strong enhancement of transmitted light through sub-wavelength holes due in part to coupling of the light with surface plasmons (Ebbesen et al. 1998) and the characterization of plasmon (Bragg) mirrors based on the back-reflection of SPs modes by a micrograting (Weeber et al. 2004). A number of applications have been reported using one or both of these designs (Brolo et al. 2004; Ferreira et al. 2009; Lesuffleur et al. 2007). Brolo and co-workers were the first to use arrays of sub-wavelength nanoholes in a gold film to monitor the binding of organic and biological molecules to a metallic surface. The technique is based on resonant surface plasmons enhanced transmission through nanoholes in a collinear optical arrangement as depicted in Fig. 4. The sensitivity was found to be 400 nm per refractive index unit. The transmission of the white light through the nanoholes induces transmission enhancement at a wavelength  $\lambda_{SPP}$  that satisfy the SP resonance conditions. Any change in the surface composition or geometry of the nanoholes is accompanied with a shift of  $\lambda_{SPP}$ .

In another work, Eftekhari et al. combined the benefits of nanofluidics and nanoplasmonics to demonstrate the possibility of SPR-based sensing using a flow-through nanohole (Eftekhari et al. 2009). The nanoholes were used in part as fluidic nanochannels to facilitate enhanced transport of reactants to the active surface, and in the other part as optical active element for analyte detection (Fig. 4). These bi-functional nanochannels offer many advantages including the confinement of both the analyte and electromagnetic field, along with the rapid diffusion of molecules at the nanoscale.

Nanohole-based SPR imaging was also investigated. The work reported by Lindquist et al. proposed a very elegant and efficient design to overcome the trade-off between the resolution and sensitivity in SPR imaging (Lindquist et al. 2009). They fabricated nanohole arrays in thin gold films at the pixel scale. Each pixel (a  $3 \times 3$  nanohole array) was surrounded by plasmonic Bragg mirrors to avoid pixel-to-pixel crosstalk and interference due to the SPs propagation length. Using this array, they successfully demonstrated the possibility of sub-micrometric multiplexed SPR imaging. Besides nanoholes, several plasmonic nanostructures are also used to improve SPR response including metallic nanowires and nanoposts (Byun et al. 2007; Malic et al. 2007).

Many designs based on nanoholes are able to overcome some of the optical and biological limitations of propagating SPR (eg. propagation length, diffusion-limited transport) and thus present a very promising approach for highly sensitive and multiplexed SPR imaging. However, the inherent uses of nanofabrication procedures currently limit the widespread application of these designs. The current fabrication is principally achieved by electron beam lithography, focused ion-beam milling, and photolithography. Some soft-lithography-based techniques are also used. A recent review of the different fabrication tools of nanostructured plasmonic materials can be found here (Henzie et al. 2009). It is obvious that the future development of nanostructure-based SPR chips is closely related to the development of rapid and cost-effective nanofabrication methods.

Another major contribution to SPR biosensors is the use of nanomaterials including metal nanoparticles, carbon nanotubes, nanowires and many other nano-objects with different size, shape and materials. Abundant literature is available in this field along with many excellent reviews (Lu et al. 2009). When light interacts with these materials or other particles much smaller than the incident wavelength, it gives rise to local oscillations of the plasmons around the nanoparticles with a frequency known as the localized surface plasmon resonance (LSPR). This phenomenon induces important electric field enhancement, leading to high detection sensitivity and enabling surface enhanced spectroscopic methods such as surface enhanced raman spectroscopy (SERS). For a more comprehensive review of these methods, the reader is directed to (Willets and Van Duyne 2007). Although LSPR has a short penetration depth of the electric field (around 20 nm) comparing to propagating modes, one of its most interesting features is the possibility of tuning the SPR intensity by varying the shape, size, composition and environment of these nano-objects (Anker et al. 2008; Hu et al. 2008; Miller and Lazarides 2005).

## 5. New materials for new possibilities

Most of the research focusing on new materials for SPR is motivated by two main considerations: obtaining films with good electric field enhancement while also presenting unique advantages with regards to surface chemistry. One of the most promising options in this field is the use of Metamaterials, particularly negative index materials (NIM) or left-handed materials. These materials exhibit simultaneously negative dielectric permittivity and magnetic permeability in a given frequency range. As a consequence, new counterintuitive phenomena are observed including negative refraction, enhancement of evanescent waves and their conversion to propagative ones (Pendry 2000; Ray et al. 2009). Therefore, surface plasmons could propagate not only in the direction parallel to the surface but in the normal direction as well. Such a behavior will significantly enhance the field depth for SPR imaging and increase the sensitivity to changes in refractive index in the bulk solution. Another interesting outcome is the possible excitation of surface plasmons polaritons by S-polarized (TE) light at the interface between a dielectric and a metamaterial (Ruppin 2000), which is impossible to implement with naturally occurring materials following Maxwell's equations. Precursor works have enabled the synthesis of metamaterials in the microwave (Shelby et al. 2001) and infrared region (Zhang et al. 2005). More important for SPR sensing are the recent efforts in the optical or visible spectral range (Burgos et al. 2010; Dolling et al. 2007; Limberopoulos et al. 2009; Shalaev et al. 2005), and the TeraHertz domain (Withayachumnankul and Abbott 2009).

Besides the wave of metamaterials, some efforts have been directed to find replacements for the resonantly active material, *i.e.* gold, the adhesive layer or even for the glass substrate. Fig. 5 depicts the wide variety of materials used in SPR chip fabrication. Rhodes et al (Rhodes et al. 2006) reported the observation of surface plasmon resonance in indium tin oxide thin film, thus demonstrating the possibility of using conducting metal oxides as active substrates for SPR biosensors in the near-infrared region. Earlier this year, conducting metal oxides (especially zinc oxide, ZnO) were also used (Chang et al. 2010) to replace Cr or Ti as adhesion layer. These two metals present a high imaginary part of the refractive index, and thus affect considerably the SP resonance properties by widening the reflectivity curve and decreasing the amplitude. Such spectral changes decrease the sensitivity of the reflectance variation and narrow the linear range (Ekgasit et al. 2005). Chang and co-workers reported that the nanocomposite ZnO/Au allowed for a sensitivity two-fold higher and a detection limit four times lower than the standard Au-based substrates. Unfortunately, they did not compare the adhesion efficiency of ZnO and Cr which is of high importance for the trade-off between adhesion and sensitivity. Also, they did not discuss the effect of the 50 nm thickness used for ZnO layer which represents around a quarter of the SP penetration



depth. Another group has recently focused on the investigation of different oxide-based thin films as protective layers to improve the chemical stability of silver SPR chips (Manesse et al. 2009). Some other efforts have been made to find replacement for the glass substrate using ceramics. Compared to BK7 slides, an order of magnitude improvement in sensitivity could be obtained using a transparent ceramic substrate with a 2.04 refractive index (Micheletto et al. 2008).

Although simulations and experiments show that these replacements improve the sensitivity, it is unlikely that the SPR community will dismiss gold and glass altogether. The good stability of gold either for deposition or surface chemistry and the cost-efficiency of glass substrates suggest these materials will remain the first choice in ATR-based SPR technology for a long time. Unlike gold and glass substrates, efforts focused on the development of new adhesion layers and sustained silver-based SPR chips are expected to increase in future. The desired SPR chip would be made of a sustained silver film with a lossless adhesion layer.

## 6. SPR-related optoelectronic components

One unique feature of biosensors and those related to SPR in particular is the multidisciplinary approach needed to create novel designs, especially with regards to instrumentation. With the help of engineers and physicists the advancement of biosensors in terms on sensitivity is being attacked not only from a surface and chip design point of view, but also that of advanced optics, light sources, and detectors.

Typically surface plasmons are excited in the Kretschmann configuration by either a light-emitting diode or laser, but recently advances in light source technology have created a new class of instrumentation based on a variety excitation sources. One recent group used a white light source for a dual-functioning SPR biosensor composed of surface plasmon microscopy (SPM) and SPR spectroscopy (Yuk et al. 2008). Using this setup SPR images and spectra were obtained from protein arrays under the same measurement environment by the dual-function SPR biosensor installed with a CCD camera and a spectrometer on a tilted angle plate. As proof-of-principle for the design, interactions of glutathione surface with glutathione S-transferase fusion proteins on arrays were analyzed by SPR image contrasts as well as by SPR spectroscopy. Also using a white light source the development of a wavelength-resolved SPR system was demonstrated recently (Chen et al. 2008) showing a very high sensitivity to low concentrations of uranyl ion from the micromolar to the picomolar range. The binding of uranyl ion to an interfacial recognition layer induces the SPR wavelength shift, permitting a sensitive detection of uranyl ion. Consequently, these results indicate that using this wavelength-resolved SPR spectroscopy system is very useful for the study of small molecular interactions.

Rather than using a different light source, the use of a radially polarized beam to excited surface plasmons has been reported (Chen and Zhan 2009). With this excitation method surface plasmons can be excited in all directions propagating to the geometric center, constructively interfering with each other and generate a strongly focused evanescent non-diffracting Bessel beam. In this work the authors demonstrate the excitation of surface plasmons on a silver-glass interface with images captured by a CCD camera. A dark ring corresponding to surface plasmon resonance excitation by a focused radially polarized beam is observed. While not applied to a biosensing platform yet, this instrumental design with the radially polarized beam offers a glimpse of a possible new light source for SPR biosensing.

Another light source that is commonly employed for SPR and SPR imaging application is a light emitting diode or LED as demonstrated in our lab and others (Suzuki et al. 2005; Wilkop et al. 2004; Yanase et al. 2010; Yang and Cho 2008). Specifically, the creation of an SPR imager using a radially polarized illumination from a LED at 530 nm to obtain speckle-

free images with high spatial resolution along all orientations was recently reported (Vander and Lipson 2009). The sensitivity to refractive index changes for a saline solution was estimated to be better than  $10^{-3}$  RIU. Another type of LED that has become more prominently used is an organic light emitting diode or OLED. One group has used an integrated OLED to create a novel SPR sensor (Frischeisen et al. 2008; Frischeisen et al. 2009). In this instrument the light emitted by the OLED leaves the prism after reflection at the sensing layer and passes a linear polarizing filter before it is focused by a collimating lens onto an optical fiber guiding it to a spectrometer. The basic functionality of the sensor was demonstrated by measuring the spectral and angle-dependent surface-plasmon dispersion at metal/air interfaces for sensing layers consisting of silver and gold with different thicknesses. As measured by refractive index changes with NaCl solutions, the instrument exhibits sensitivity on par with commercial instruments.

Not only can new light sources be used for enhanced sensitivity or resolution, but they can also be used for speed of data acquisition. Recently the development of a novel technique that has the potential to realize interrogation of SPR sensors at very high speed was reported (Zheng et al. 2008). A broadband coherent laser generating short optical pulses at a high repetition rate is used along with a highly dispersive optical element to obtain fast data acquisition. In their setup the change in pulse shape over time is measured with a photodetector. The SPR response could be acquired for each pulse with data acquisition conceivably possible at a rate of tens of MHz, vastly improving current SPR techniques. By measuring the variations in the pulse shapes of the chirped pulses, sensitive SPR measurements in PBS buffer were made to demonstrate the utility of this apparatus.

Additionally, beyond acquisition speed and sensor sensitivity, recently a group utilized an untapped area of the electromagnetic spectrum by the advent of the first SPR sensor in the mid-infrared range (Herminjard et al. 2009). Surface plasmons are excited on a Ti/Au substrate deposited on a CaF<sub>2</sub> prism where light excitation is provided by a quantum cascade laser (QCL) source. Evidence of SPR is presented by detecting CO<sub>2</sub> and N<sub>2</sub> mixtures as test samples. Due to the absorption of CO<sub>2</sub> at this wavelength in the mid-IR, it is shown that the sensitivity of this configuration is five times higher than a similar SPR sensor operating in the visible range of the spectrum. This instrument represents a promising detection tool for numerous gaseous molecules that absorb in the IR region.

Another area of great interest, especially for engineers, is the development of new SPR or SPR imaging instruments. Due to the low flexibility and limited possibilities offered by commercially available SPR imagers for sensor development, many groups (including ours) choose to build their own instruments. Among the most interesting developments in the last few years includes a two-dimensional phase-detection system for a SPR imaging (Lee et al. 2008). The sensor utilizes polarization interferometry to detect phase differences between the s and p polarizations. This instrument can successfully detect a spatial phase-difference variation in a 1 mm<sup>2</sup> area with a sensitivity of  $4.3 \times 10^{-6}$  RIU using PBS buffer as a calibration standard. Another similar instrument has been reported using polarization interferometry (Yu et al. 2008a; Yu et al. 2008b). The authors noted the complete common-light path detection method can restrain light noise and improve detection sensitivity. For sensitivity determination various concentrations of NaCl solutions were used indicating a sensitivity of  $10^{-6}$  refractive index units (RIU).

There is also evidence of slightly different experimental protocols for obtaining SPR imaging data can lead to enhanced sensitivity. Specifically, the detection limit of SPR measurements could be improved by a factor of 2–3.5 if the angle of incidence is near the reflection minimum of the SPR resonance curve instead at the position of the steepest slope, the standard alignment in SPR imaging (Zybin et al. 2007). The enhancement of the

detection power, a result of signal-to-noise (S/N) optimization, is demonstrated by applying a photodiode and a CCD camera for SPR detection while using NaCl solutions as calibrants. More instrumental optimization has been reported by Mirsky and co-workers who report enhanced analytical performance of SPR imaging by splitting a macroscopic sensing surface into multiple microscopic neighboring sensing and referencing subareas (Boecker et al. 2008). Their data indicates multiple referencing reduces intensity fluctuations across the total sensing area and, therefore, improves the S/N ratio proportional to the splitting factor. This data acquisition method is demonstrated by examining the biotin/streptavidin interaction resulting in enhanced sensitivity. Specifically, an effective variation of the reflected intensity of about  $10^{-4}$ , which corresponds to the refraction index variation of  $3 \times 10^{-6}$ , was detected with S/N ratio about 10 without any temperature stabilization of the sensing area. These are just a few of instrumental enhancements that could lead to remarkable improvement in terms of SPR imaging and spectroscopy sensitivity in the future.

## 7. Combining SPR with other analytical techniques

The combination of surface plasmon resonance with complementary analytical techniques has become increasingly popular during the last decade. The hyphenation could be divided into two different approaches depending on research emphasis: 1) combining different physical phenomena in the same instrument in order to achieve a higher sensitivity and/or resolution; and 2) achieving serial use of different instruments for the same sample analysis.

One of the most popular examples of the first approach is surface enhanced Raman spectroscopy. This technique enables an unprecedented spectroscopic signal enhancement on the order of  $10^6$  for the detection of single molecules (Nie and Emory 1997). Similar to SERS technique, surface-plasmon field-enhanced fluorescence spectroscopy enhances the sensitivity by several orders of magnitude (ca.  $10^3$ ) (Liebermann and Knoll 2000). The concept is based on the excitation by surface plasmons of fluorescently labeled analyte molecules, and detection of the emitted fluorescence intensity. SPR-ellipsometry is also reported to increase the sensitivity by one or two orders of magnitude for thin film analysis while also enabling measurements in opaque liquids (Arwin et al. 2004).

The serial use of different analytical instruments with SPR biosensors is generally utilized to speed up and complement the bioanalysis procedure. This approach is well illustrated by the successful and rapid implementation of SPR-mass spectrometry (MS) (Nelson et al. 1997). It is based on the use of SPR to characterize the activity of a target molecule, which is then recovered from the SPR chip surface for a subsequent MS analysis. Such a sequence enables the rapid study of both the function (by SPR) and the structure (by MS) of partner molecules. We recently demonstrated that an ultrathin calcinated film on a gold SPR substrate allows effective laser desorption/ionization MS analysis of proteins and peptides without the need of an organic matrix (Duan et al. 2010). Another interesting design involves the development of one single chip to combine micro-free flow electrophoresis ( $\mu$ -FFE) and surface plasmon resonance detection (Kohlheyer et al. 2006). The combination of this technique with MS analysis represents one of the most interesting sequences towards a unique proteomics platform (Fig. 6). Other techniques have been recently coupled to SPR-MS including liquid chromatography (Visser et al. 2007) and protein digestion by immobilized enzymes reactors (Stigter et al. 2009). Scanning tunneling microscopy (STM) and atomic force microscopy (AFM) has also been used to correlate the attachment and positioning of biomolecules onto the surface with their functionality measured by an SPR biosensor (Davies et al. 1994), and for simultaneous analysis of thin films and polymers (Baba et al. 2006; Shakesheff et al. 1995). The optical set-up for AFM-SPR could be easily implemented due to the geometrical compatibility (the AFM tip probes the sample from the top while the incident light of ATR-SPR reaches the surface from underneath). Moreover, it

could be combined to additional devices such as electrochemical instrumentation (Baba et al. 2006). Other recent combinations include surface acoustic wave sensor (Bender et al. 2009; Francis et al. 2006; Galopin et al. 2007), HPLC (Du and Zhou 2008), and quartz crystal microbalance (QCM) (Kim et al. 2010).

## 8. Challenges and future trends

The main challenges that face surface plasmon resonance-based sensors research in coming years, in our opinion, could be summarized in six future directions: 1) The hyphenation approaches or serial multi-analytical combinations are likely to reach a plateau because of the compatibility issues, complimentary requirements and a limited number of configurations. One exception to this trend is SPR-MS, which is increasingly used in proteomics to adequately determine the structure-function relationship in one assay. We expect this combination to be expanded to other separation technologies, making additional steps towards a complete label-free proteomics platform. 2) Beyond the serial use of instruments, an interesting development will most likely concern the exploitation of both the SPR phenomenon and platform to improve the sensing capabilities of traditional spectroscopic and imaging techniques. In other words, rather than a sequential use of different devices, the physics of SPR will be combined with other physical phenomena for reciprocal signal conversion or enhancement. SPR-TeraHertz imaging (Miyamaru et al. 2007), scanning probe microscopy techniques (Kawata et al. 2009) and electrochemical methods (Shan et al. 2010) are the most recent examples of this evolution. 3) A promising development is the implementation of metamaterials in the visible frequencies. Although the expanded use of these materials is currently limited by their costly and time-consuming fabrication, the development of affordable nanofabrication techniques will open up their application to the entire field of electromagnetic waves-based detection technologies. 4) The microfluidic and bio-microsystem technologies represent a very effective and promising tool for multiplexed and automated analysis, particularly for SPR imaging. A continuous development is expected in this field. Furthermore, we expect the application of SPR sensing in micro- and nanofluidics. This means that SPR imaging could be used to investigate fluid dynamics including mixing experiments and flows at the micro/nanoscale (Kim and Kihm 2010). 5) Besides new chip design and optical platform developments, new efforts will be dedicated in the future to reduce the noise originating from the optoelectronic components (light sources and detectors) associated with the SPR experiments. Recent theoretical predictions suggest that the optoelectronic-generated noise is one of the major limitations of SPR instrument sensitivity (Piliarik and Homola 2009). 6) Finally, the fundamental research on the surface plasmon behavior at the nanoscale will continue to attract increasing attention and funding as the impact of such studies is already reaching several important fields including photonics, optoelectronics and energy. As a side effect, surface plasmon resonance-based sensors will largely benefit from this tendency.

## Acknowledgments

The authors gratefully acknowledge the financial support of the US National Science Foundation (CHE-0719224) and the National Institute of Health (1R21EB-009551).

## References

- Abbas A, Dargent T, Croix D, Salzet M, Bocquet B. *Medical Science Monitor*. 2009a; 15:Mt121–Mt125. [PubMed: 19721407]
- Abbas A, Treizebre A, Supiot P, Bourzgui NE, Guillochon D, Vercaigne-Marko D, Bocquet B. *Biosensors & Bioelectronics*. 2009b; 25:154–160. [PubMed: 19608402]
- Abdulhalim I, Zourob M, Lakhtakia A. *Electromagnetics*. 2008; 28:214–242.

- Amarie D, Alileche A, Dragnea B, Glazier JA. *Analytical Chemistry*. 2010; 82:343–352. [PubMed: 19968248]
- Anker JN, Hall WP, Lyandres O, Shah NC, Zhao J, Van Duyne RP. *Nat Mater*. 2008; 7:442–453. [PubMed: 18497851]
- Arwin H, Poksinski M, Johansen K. *Applied Optics*. 2004; 43:3028–3036. [PubMed: 15176189]
- Baba A, Knoll W, Advincula R. *Review of Scientific Instruments*. 2006; 77:064101.
- Bender F, Roach P, Tsortos A, Papadakis G, Newton MI, McHale G, Gizeli E. *Measurement Science & Technology*. 2009; 20:124011.
- Boecker D, Zybin A, Niemax K, Grunwald C, Mirsky VM. *Review of Scientific Instruments*. 2008; 79:023110. [PubMed: 18315286]
- Brolo AG, Gordon R, Leathem B, Kavanagh KL. *Langmuir*. 2004; 20:4813–4815. [PubMed: 15984236]
- Burgos SP, de Waele R, Polman A, Atwater HA. *Nature Materials*. 2010; 9:407–412.
- Byun KM, Yoon SJ, Kim D, Kim SJ. *Optics Letters*. 2007; 32:1902–1904. [PubMed: 17603608]
- Chang CC, Chiu NF, Lin DS, Chu-Su Y, Liang YH, Lin CW. *Analytical Chemistry*. 2010; 82:1207–1212. [PubMed: 20102177]
- Chen H, Lee Y, Oh MC, Lee J, Ryu SC, Hwang YH, Koh K. *Sensors and Actuators B (Chemical)*. 2008; 134:419–422.
- Chen, W.; Zhan, Q. *Proceedings of the SPIE - The International Society for Optical Engineering* 71920A; 2009. p. 71910
- Chien FC, Chen SJ. *Biosensors & Bioelectronics*. 2004; 20:633–642. [PubMed: 15494249]
- Davies J, Roberts CJ, Dawkes AC, Sefton J, Edwards JC, Glasbey TO, Haymes AG, Davies MC, Jackson DE, Lomas M, Shakesheff KM, Tendler SJB, Wilkins MJ, Williams PM. *Langmuir*. 1994; 10:2654–2661.
- Dolling G, Wegener M, Soukoulis CM, Linden S. *Optics Letters*. 2007; 32:53–55. [PubMed: 17167581]
- Dong Y, Wilkop T, Xu D, Wang Z, Cheng Q. *Analytical and Bioanalytical Chemistry*. 2008; 390:1575–1583. [PubMed: 18251014]
- Du M, Zhou FM. *Analytical Chemistry*. 2008; 80:4225–4230. [PubMed: 18457411]
- Duan J, Linman MJ, Cheng Q. *Analytical Chemistry*. 2010; 82:5088–5094. [PubMed: 20496922]
- Ebbesen TW, Lezec HJ, Ghaemi HF, Thio T, Wolff PA. *Nature*. 1998; 391:667–669.
- Eddings MA, Eckman JW, Arana CA, Papalia GA, Connolly JE, Gale BK, Myszkowski DG. *Analytical Biochemistry*. 2009; 385:309–313. [PubMed: 19059374]
- Eftekhari F, Escobedo C, Ferreira J, Duan X, Giroto EM, Brolo AG, Gordon R, Sinton D. *Analytical Chemistry*. 2009; 81:4308–4311. [PubMed: 19408948]
- Ekgasit S, Thammacharoen C, Knoll W. *Analytical Chemistry*. 2004; 76:561–568. [PubMed: 14750847]
- Ekgasit S, Thammacharoen C, Yu F, Knoll W. *Applied Spectroscopy*. 2005; 59:661–667. [PubMed: 15969812]
- Ferreira J, Santos MJ, Rahman MM, Brolo AG, Gordon R, Sinton D, Giroto EM. *Journal of the American Chemical Society*. 2009; 131:436–437. [PubMed: 19140784]
- Francis LA, Friedt JM, Zhou C, Bertrand P. *Analytical Chemistry*. 2006; 78:4200–4209. [PubMed: 16771551]
- Frischeisen J, Mayr C, Reinke NA, Nowy S, Brutting W. *Optics Express*. 2008; 16:18426–18436. [PubMed: 18958121]
- Frischeisen J, Reinke NA, Brutting W. *Laser Focus World*. 2009; 45:57–60.
- Galopin E, Beaugeois M, Pinchemel B, Camart JC, Bouazaoui M, Thomy V. *Biosensors & Bioelectronics*. 2007; 23:746–750. [PubMed: 17884436]
- Gordon JG, Swalen JD. *Optics Communications*. 1977; 22:374–376.
- Grant, J.; Shia, X.; Altonb, J.; Cumminga, DRS. *IEEE Photonics Society, Winter Topicals Meeting Series*. 2010. p. 34-35.



- Hassani A, Dupuis A, Skorobogatiy M. *Journal of the Optical Society of America B-Optical Physics*. 2008; 25:1771–1775.
- Henzie J, Lee J, Lee MH, Hasan W, Odom TW. *Annual Reviews of Physical Chemistry*. 2009; 60:147–165.
- Herminjard S, Sirigu L, Herzig HP, Studemann E, Crottini A, Pellaux JP, Gresch T, Fischer M, Faist J. *Optics Express*. 2009; 17:293–303. [PubMed: 19129898]
- Hibbins AP, Sambles JR, Lawrence CR. *Journal of Applied Physics*. 1999; 86:1791–1795.
- Hiep HM, Nakayama T, Saito M, Yamamura S, Takamura Y, Tamiya E. *Japanese Journal of Applied Physics*. 2008; 47:1337–1341.
- Hoa XD, Kirk AG, Tabrizian M. *Biosensors & Bioelectronics*. 2007; 23:151–160. [PubMed: 17716889]
- Homola J. *Chemical Reviews*. 2008; 108:462–493. [PubMed: 18229953]
- Hornauer D, Kapitza H, Raether H. *Journal of Physics D-Applied Physics*. 1974; 7:L100–L102.
- Hu M, Novo C, Funston A, Wang H, Staleva H, Zou S, Mulvaney P, Xia Y, Hartland GV. *Journal of Material Chemistry*. 2008; 18:1949–1960.
- Huang C, Bonroy K, Reekmans G, Laureyn W, Verhaegen K, De Vlaminck I, Lagae L, Borghs G. *Biomedical Microdevices*. 2009; 11:893–901. [PubMed: 19353272]
- Jen YJ, Liao YH. *Applied Physics Letters*. 2009; 94:011105–3.
- Kapitza H. *Optics Communications*. 1976; 16:73–75.
- Kawata S, Inouye Y, Verma P. *Nature Photonics*. 2009; 3:388–394.
- Kim I, Kihm KD. *Optics Letters*. 2010; 35:393–395. [PubMed: 20125732]
- Kim M, Kim SH, Ohashi T, Muramatsu H, Chang SM, Kim WS. *Bioprocess and Biosystem Engineering*. 2010; 33:39–45.
- Kocabas A, Dana A, Aydinli A. *Applied Physics Letters*. 2006; 89:041123.
- Kohlheyer D, Besselink GAJ, Schlautmann S, Schasfoort RBM. *Lab on a Chip*. 2006; 6:374–380. [PubMed: 16511620]
- Kovacs GJ, Scott GD. *Physical Review B*. 1977; 16:1297–1311.
- Kretschmann E, Raether H. *Zeitschrift Fur Naturforschung Part a-Astrofysik Physik Und Physikalische Chemie A*. 1968a; 23:615.
- Kretschmann E, Raether H. *Zeitschrift Fur Naturforschung Part a-Astrofysik Physik Und Physikalische Chemie A*. 1968b; 23:2135.
- Krishnamoorthy G, Carlen ET, deBoer HL, van den Berg A, Schasfoort RB. *Analytical Chemistry*. 2010; 82:4145–4150. [PubMed: 20402468]
- Lau KHA, Tan LS, Tamada K, Sander MS, Knoll W. *Journal of Physical Chemistry B*. 2004; 108:10812–10818.
- Lee JY, Chou TK, Shih HC. *Optics Letters*. 2008; 33:434–436. [PubMed: 18311283]
- Lee KH, Su YD, Chen SJ, Tseng FG, Lee GB. *Biosensors & Bioelectronics*. 2007; 23:466–472. [PubMed: 17618110]
- Lesuffleur A, Im H, Lindquist NC, Oh SH. *Applied Physics Letters*. 2007; 90:243, 110.
- Liebermann T, Knoll W. *Colloids and Surfaces a-Physicochemical and Engineering Aspects*. 2000; 171:115–130.
- Liedberg B, Nylander C, Lundstrom I. *Sensors and Actuators*. 1983; 4:299–304.
- Limberopoulos N, Akyurtlu A, Higginson K, Kussow AG, Merritt CD. *Applied Physics Letters*. 2009; 95:023306.
- Lindquist NC, Lesuffleur A, Im H, Oh SH. *Lab Chip*. 2009; 9:382–387. [PubMed: 19156286]
- Liu J, Eddings MA, Miles AR, Bukasov R, Gale BK, Shumaker-Parry JS. *Analytical Chemistry*. 2009; 81:4296–4301. [PubMed: 19408947]
- Lo SZA, Murphy TE. *Applied Physics Letters*. 2010; 96:201104.
- Lu X, Rycenga M, Skrabalak SE, Wiley B, Xia Y. *Annu Rev Phys Chem*. 2009; 60:167–192. [PubMed: 18976140]
- Luo Y, Yu F, Zare RN. *Lab on a Chip*. 2008; 8:694–700. [PubMed: 18432338]



- Malic L, Cui B, Veres T, Tabrizian M. *Optics Letters*. 2007; 32:3092–3094. [PubMed: 17975607]
- Malic L, Veres T, Tabrizian M. *Biosensors & Bioelectronics*. 2009a; 24:2218–2224. [PubMed: 19136248]
- Malic L, Veres T, Tabrizian M. *Lab on a Chip*. 2009b; 9:473–475. [PubMed: 19156299]
- Manesse M, Sanjines R, Stambouli V, Jorel C, Pelissier B, Pisarek M, Boukherroub R, Szunerits S. *Langmuir*. 2009; 25:8036–8041. [PubMed: 19594181]
- McMillan BG, Berlouis LEA, Cruickshank FR, Pugh D, Brevet PF. *Applied Physics Letters*. 2005; 86:211912.
- Mertens H, Verhoeven J, Polman A, Tichelaar FD. *Applied Physics Letters*. 2004; 85:1317–1319.
- Micheletto R, Hamamoto K, Fujii T, Kawakami Y. *Applied Physics Letters*. 2008; 93:174104.
- Miller MM, Lazarides AA. *J Phys Chem B*. 2005; 109:21556–21565. [PubMed: 16853799]
- Miyamaru F, Takeda MW, Suzuki T, Otani C. *Optics Express*. 2007; 15:14804–14809. [PubMed: 19550760]
- Natarajan S, Katsamba PS, Miles A, Eckman J, Papalia GA, Rich RL, Gale BK, Myszka DG. *Analytical Biochemistry*. 2008; 373:141–146. [PubMed: 17868635]
- Nelson RW, Krone JR, Jansson O. *Analytical Chemistry*. 1997; 69:4363–4368. [PubMed: 9360491]
- Nie S, Emory SR. *Science*. 1997; 275:1102–1106. [PubMed: 9027306]
- Otto A. *Z Phys*. 1968; 216:398–410.
- Ouellet E, Lausted C, Lin T, Yang CW, Hood L, Lagally ET. *Lab on a Chip*. 2010; 10:581–588. [PubMed: 20162233]
- Palomba S, Novotny L. *Physical Review Letters*. 2008; 101:056802. [PubMed: 18764416]
- Pendry JB. *Physical Reviews Letters*. 2000; 85:3966–3969.
- Pendry JB, Martin-Moreno L, Garcia-Vidal FJ. *Science*. 2004; 305:847–848. [PubMed: 15247438]
- Phillips KS, Cheng Q. *Analytical and Bioanalytical Chemistry*. 2007; 387:1831–1840. [PubMed: 17203259]
- Piliarik M, Homola J. *Optics Express*. 2009; 17:16505–16517. [PubMed: 19770865]
- Raether, H. *Surface plasmons on smooth and rough surfaces and on gratings*. Springer-Verlag; Berlin: 1988.
- Ray EA, Hampton MJ, Lopez R. *Optics Letters*. 2009; 34:2048–2050. [PubMed: 19571995]
- Rhodes C, Franzen S, Maria JP, Losego M, Leonard DN, Laughlin B, Duscher G, Weibel S. *Journal of Applied Physics*. 2006; 100:054905.
- Ruppin R. *Phys Lett A*. 2000; 277:61–64.
- Salamon Z, Macleod HA, Tollin G. *Biophysical Journal*. 1997; 73:2791–2797. [PubMed: 9370473]
- Salamon Z, Tollin G. *Biophysical Journal*. 2001; 80:1557–1567. [PubMed: 11222316]
- Sarid D. *Physical Review Letters*. 1981; 47:1927–1930.
- Scarano S, Mascini M, Turner AP, Minunni M. *Biosensors & Bioelectronics*. 2010; 25:957–966. [PubMed: 19765967]
- Shakesheff KM, Chen XY, Davies MC, Domb A, Roberts CJ, Tendler SJB, Williams PM. *Langmuir*. 1995; 11:3921–3927.
- Shalaev VM, Cai WS, Chettiar UK, Yuan HK, Sarychev AK, Drachev VP, Kildishev AV. *Optics Letters*. 2005; 30:3356–3358. [PubMed: 16389830]
- Shan X, Patel U, Wang S, Iglesias R, Tao N. *Science*. 2010; 327:1363–1366. [PubMed: 20223983]
- Shelby RA, Smith DR, Schultz S. *Science*. 2001; 292:77–79. [PubMed: 11292865]
- Springer T, Piliarik M, Homola J. *Sensors and Actuators B-Chemical*. 2010; 145:588–591.
- Stigter ECA, de Jong GJ, van Bennekom WP. *Biosensors & Bioelectronics*. 2009; 24:2184–2190. [PubMed: 19157843]
- Suzuki A, Kondoh J, Matsui Y, Shiokawa S, Suzuki K. *Sensors and Actuators B-Chemical*. 2005; 106:383–387.
- Tan PS, Yuan XC, Lin J, Wang Q, Mei T, Burge RE, Mu GG. *Applied Physics Letters*. 2008; 92:111108.

- Taylor JD, Linman MJ, Wilkop T, Cheng Q. *Analytical Chemistry*. 2009; 81:1146–1153. [PubMed: 19178341]
- Taylor JD, Phillips KS, Cheng Q. *Lab on a Chip*. 2007; 7:927–930. [PubMed: 17594015]
- Telezhnikova O, Homola J. *Optics Letters*. 2006; 31:3339–3341. [PubMed: 17072416]
- Treizebre A, Bocquet B. *International Journal of Nanotechnology*. 2008; 5:784–795.
- Treizebre A, Bocquet B, Xu YS, Bosisio RG. *Microwave and Optical Technology Letters*. 2008; 50:2998–3001.
- Vander R, Lipson SG. *Optics Letters*. 2009; 34:37–39. [PubMed: 19109632]
- Visser NF, Scholten A, van den Heuvel RH, Heck AJ. *Chembiochem*. 2007; 8:298–305. [PubMed: 17206730]
- Wang Z, Wilkop T, Xu D, Dong Y, Ma G, Cheng Q. *Analytical and Bioanalytical Chemistry*. 2007; 389:819–825. [PubMed: 17673982]
- Weeber JC, Lacroute Y, Dereux A, Devaux E, Ebbesen T, Girard C, González MU, Baudrion AL. *Physical Review B*. 2004; 70:235406.
- Wilkop T, Wang ZZ, Cheng Q. *Langmuir*. 2004; 20:11141–11148. [PubMed: 15568869]
- Willets KA, Van Duyne RP. *Annual Reviews of Physical Chemistry*. 2007; 58:267–297.
- Williams, M., , 11, 3921–3927., 1995. *Langmuir*.
- Withayachumnankul W, Abbott D. *IEEE Photonics J*. 2009; 1:99–118.
- Wood RW. *Proc Phys Soc London*. 1902; 18:166–182.
- Xiaohua S, Clearya A, Khalida A, Cumminga DRS. *Microelectronic Engineering*. 2009; 86:1111–1113.
- Yanase Y, Araki A, Suzuki H, Tsutsui T, Kimura T, Okamoto K, Nakatani T, Hiragun T, Hide M. *Biosensors & Bioelectronics*. 2010; 25:1244–1247. [PubMed: 19880304]
- Yang G, Cho NH. *Food Science and Biotechnology*. 2008; 17:1038–1046.
- Yu X, Ding X, Liu F, Wei X, Wang D. *Measurement Science & Technology*. 2008a; 19:015301.
- Yu XL, Ding X, Liu FF, Deng Y. *Sensors and Actuators B-Chemical*. 2008b; 130:52–58.
- Yuk JS, Jung JW, Kim YM, Ha KS. *Sensors & Actuators: B Chemical*. 2008; 129:113–119.
- Zhang DG, Yuan XC, Bouhelier A, Wang P, Ming H. *Optics Letters*. 2010; 35:408–410. [PubMed: 20125737]
- Zhang S, Fan WJ, Malloy KJ, Brueck SRJ, Panoiu NC, Osgood RM. *Optics Express*. 2005; 13:4922–4930. [PubMed: 19498480]
- Zheng Z, Wan Y, Zhao X, Zhu J. *Sensors and Actuators B-Chemical*. 2008; 133:671–676.
- Zordan, MD.; Grafton, MMG.; Kinam, P.; Leary, JF. *Proceeding of SPIE*; 2010. p. 7553
- Zybin A, Boecker D, Mirsky VM, Niemax K. *Analytical Chemistry*. 2007; 79:4233–4236. [PubMed: 17451227]

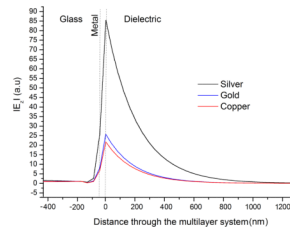


**Fig. 1.** Electric field ( $E_z$ ) distribution in the direction normal to the metal-dielectric interface during surface plasmon resonance. The normalized  $E_z$  intensity as a function of the distance from the interface shows the field enhancement and the exponential decay at 650 nm excitation wavelength for three metals: silver (50 nm;  $n=0.0666+ i 4.045$ ), gold (50 nm;  $n=0.180+ i 3.55$ ) and copper (50 nm;  $n=0.22+ i 3.54$ ). The dielectric medium is water ( $n=1.333$ ).

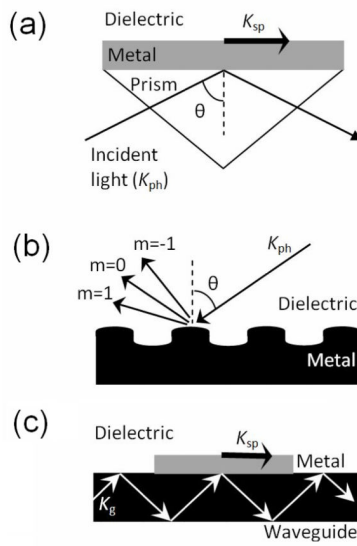


**Fig. 2.** Coupling schemes of incident light to surface plasmons: (a) prism coupling, (b) grating coupling, and (c) waveguide coupling. ( $K_{ph}$ : wave vector of the incident light,  $K_{sp}$ : wave vector of the surface plasmons,  $K_g$ : wave vector of the guided mode,  $\Lambda$ : periodicity of the grating,  $m$ : diffraction order).

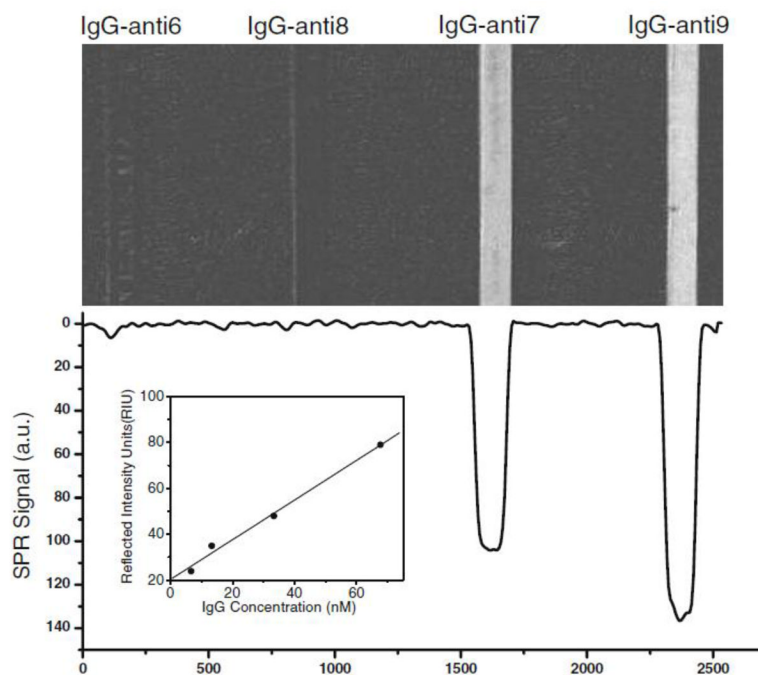


**Fig. 3.** SPR image of the interaction of different antibodies with human IgG inside the microchannels (top) and cross-sectional line profile (bottom). From left to right: IgG-anti6, IgG-anti8, IgG-anti7 and IgG-anti9. The inset is the calibration curve for IgG anti9 (Figure reproduced with permission from Dong et al., 2008).

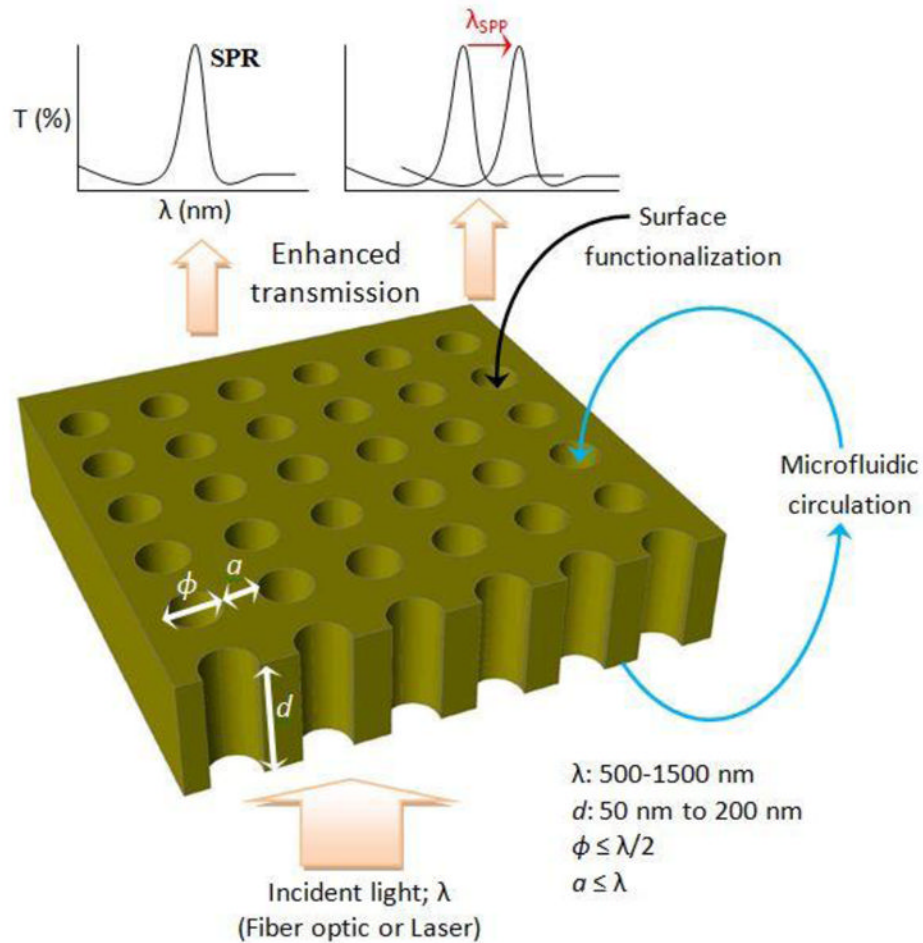


**Fig. 4.** Sub-wavelength Nanoholes array for SPR biosensing. The nanoholes are fabricated in a metal layer (Au, Ag or Al) deposited on a quartz or glass slide or perforated silicon nitride membrane to enable the flow through the nanoholes. The detection is performed in transmission mode (collinear optics) for SPR spectroscopy or microscopy. The values indicated for gold thickness  $d$ , the nanohole diameter  $\phi$ , the periodicity  $a$ , and the incident wavelength  $\lambda$  represent the most used parameters in the literature.



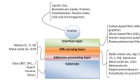


**Fig. 5.**  
Different materials used in SPR-based chips.

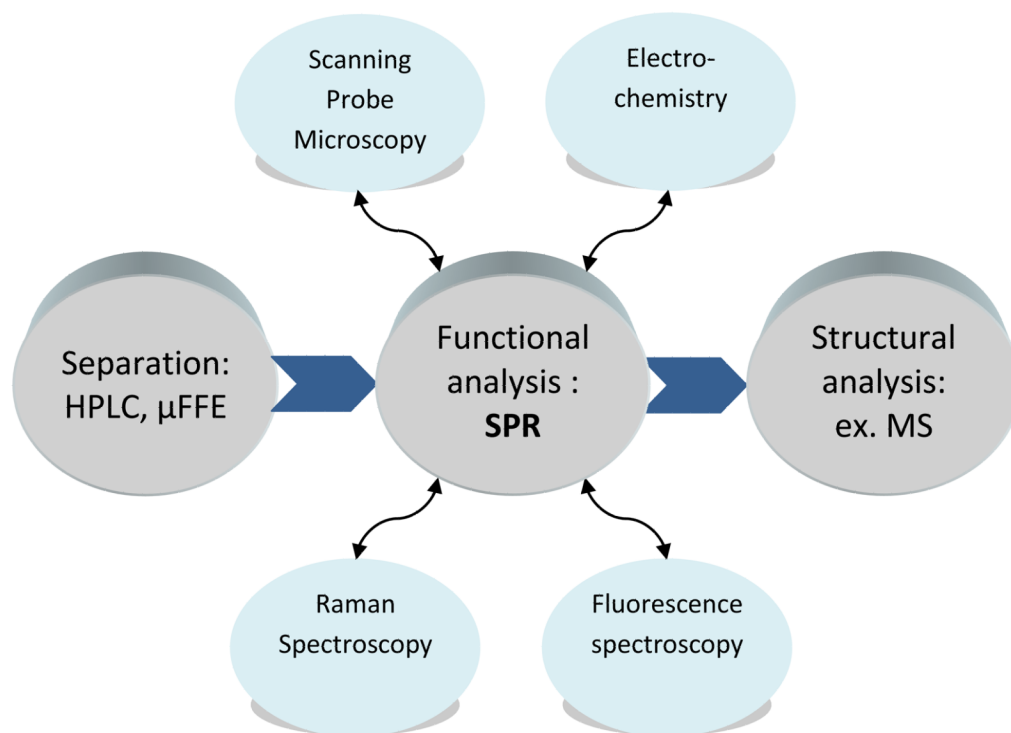


**Fig. 6.** Hyphenation approach of SPR technology. The thick unidirectional arrows show the serial use of different analytical instruments. The HPLC/ $\mu$ FFE-SPR-MS sequence represents one of the most relevant combinations. The thin bidirectional arrows represent the exploitation of surface plasmons resonance phenomenon by another analytical technique.

**Table 1**

Planar configurations of ATR-based SPR biosensors. Cross-dashed area: SPR-carrying metal, blank area: dielectric layer, gray triangle: prism, dotted area: dielectric waveguiding layer. The black small triangles show the interface at which surface plasmon resonance occur, while the black circles show a propagating waveguide mode resonance.

Nomenclature	Design	Related Reference
Otto configuration		A. Otto, 1968
Kretschmann configuration		Kretschmann, 1971
long-range SPR (LRSPR)		Sarid, 1981
Plasmon-waveguide resonance (PWR)		Salamon et al., 1997
waveguide-coupled SPR (WCSPR).		Kovacs and Scott, 1977, 1978